Sorting motile rods by activity

Nitin Kumar[1*], Harsh Soni[1,2†], Rahul Kumar Gupta[2], Sriram Ramaswamy[2,‡] and A.K. Sood[1]
[1] *Department of Physics, Indian Institute of Science, Bangalore 560 012, India and*
[2] *TIFR Centre for Interdisciplinary Sciences, Tata Institute of Fundamental Research, 21 Brundavan Colony, Osman Sagar Road, Narsingi, Hyderabad 500 075, India*[‡]
(Dated: March 30, 2016)

We show, through experiments and simulations, that geometrically polar granular rods, rendered active by the transduction of vertical vibration, undergo a collective trapping phase transition in the presence of a V-shaped obstacle when the opening angle drops below a threshold value. We propose a mechanism that accounts qualitatively for the transition, based on the cooperative reduction of angular noise with increasing area fraction. We exploit the sensitivity of trapping to the persistence of directed motion to sort particles based on the statistical properties of their activity.

PACS numbers: 45.70. -n, 05.40.-a, 05.70.Ln, 45.70.Vn

arXiv:1603.08535v1 [cond-mat.soft] 28 Mar 2016

The interplay of directed energy transduction and interparticle interaction gives rise to a host of dramatic self-organizing effects in collections of active particles [1, 2]. Although the active matter paradigm was formulated to describe the living state, it is frequently more practical to study this class of systems by creating faithful imitations [3–7]. Here we work with fore-aft asymmetric metal rods, millimeters in length, confined in a quasi 2D geometry and rendered motile in the horizontal plane by vertical vibration. Such objects, which we shall refer to as active polar rods [3, 7–9] are now a standard test-bed for probing the collective [7] and single-particle [10, 11] statistical physics of self-driven matter. The dynamics of self-propelled particles is influenced by the shape of the confining boundary, often leading to clustering and trapping [12, 13]. Such effects could have practical consequences in the industrial processing of granular material through their influence on transport through narrow channels. Experiments with self-propelled granular particles have shown that clustering at the periphery can be minimized through the use of scalloped boundaries whose curvature reinjects particles into the interior [7, 14, 15]. However, a closer exploration of the interaction of active particles with boundaries and obstacles is called for.

In this Letter we investigate, experimentally and numerically, the collective dynamics of mono- and bidisperse collections of active polar rods in the presence of a V-shaped trap, as a function of the angle θ of the V and the nature of fluctuations in the motion of a single rod. In experiments the latter is governed by particle shape, while in simulations it can be varied continuously. Our results are as follows. (i) Particles with strongly directed motion are trapped for $\theta \lesssim 120^\circ$, consistent with the active Brownian studies of [16] (Fig. 1, top panel). In particular, we offer evidence to the effect that the onset of trapping has the character of a phase transition. (ii) Most interesting is the *sorting* function of the trap: when placed in a homogeneous bidisperse mixture it rejects particles with noisy motion and collects those with persistent motility (Fig. 1, bottom panel). The idea that a passive enclosure can spontaneously sort [17] active particles based on the statistical characteristics of their motion suggests new directions for isolating motile cells or bacteria of different types.

We now describe our findings in detail. Our experiments are carried out in a shallow circular geometry with 13 cm diameter [10] and a flower shaped cell wall in order to avoid clustering [7]. It is covered by a glass lid at 1.2 mm above the surface, thus forming a confined two-dimensional system. We work with geometrically polar brass rods of length $\ell = 4.5$ mm and diameter 1.1 mm at the thick end. The cell is fixed on a permanent-magnet shaker (LDS V406-PA 100E) which drives the plate sinusoidally in the vertical direction with amplitude a_0 and frequency f= 200 Hz, corresponding to dimensionless shaking strength $\Gamma \equiv a_0(2\pi f)^2/g = 7.0$, where g is the acceleration due to gravity. The rod transduces the vibration into predominantly forward motion in the direction of its pointed end (supplementary video 1). A high-speed camera (Redlake MotionPro X3) records the dynamics of the particles and ImageJ [18] is used to extract instantaneous position, orientation and velocity of the rods.

We use V-shaped traps of aluminium with arm length $L = 10\ell \simeq 4.5$ cm with $20^\circ \leq \theta \leq 160^\circ$ in steps of 10°. The trap is placed in the middle of the cell and stuck to the surface with double-sided tape. The cell is filled by a layer of rods spread homogeneously and isotropically on the surface. All experiments on the trapping in monodisperse systems are done with the number of rods fixed at 150.

Mechanically faithful simulations, with details as in [7], are conducted to investigate which properties of individual particles govern their propensity to get trapped

*Presently at: James Franck Institute, University of Chicago, Chicago, Illinois 60637, USA
†Current address: School of Engineering, Brown University, Providence 02912, USA

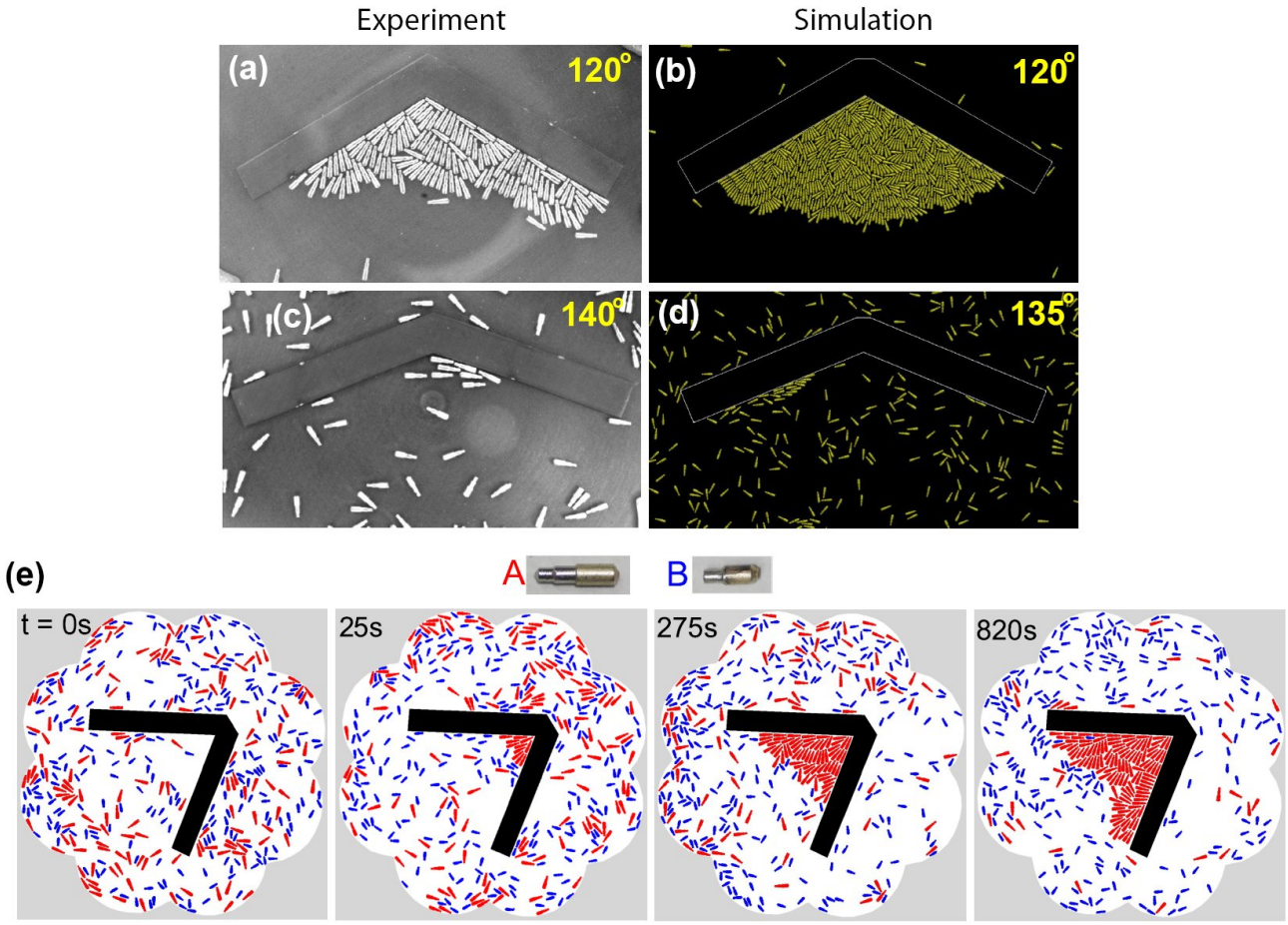

FIG. 1: (a, b, c, d) A typical trapped and untrapped states in experiment and simulation. The angles are mentioned in yellow. The system size, in terms of rod length, is 20 and 39 in experiment and simulation respectively. (e) A sequence of images showing separation of polar particles based on their activity with only particle A getting trapped.

and, hence, which features control activity-based sorting. We construct the tapered rods as arrays of overlapping spheres of different sizes [7]. Vibrating base and lid are represented by two hard horizontal walls whose vertical (z) positions at time t are $\mathcal{A}\cos 2\pi ft$ and $\mathcal{A}\cos 2\pi ft + w$ respectively. In our simulations we work at $\phi_r/F = 1.2$, where ϕ_r is rod area fraction and F is the ratio of trap area $A_t = L^2 \sin\theta/2$ to that of the base, to ensure that the trap does not trivially exhaust the the total number of rods available on the base plate. We choose periodic boundary conditions in the xy plane with linear dimensions of 19.3ℓ, consistent with the experimental geometry. We also run simulations at larger system sizes, always at $\phi_r/F = 1.2$. Surface imperfections cause the rods in the experiments to perform rotational diffusion, which we capture in the simulation [7] by supplying a random angular velocity, $\omega_z = \varepsilon v_{rel}$ where $\varepsilon = \pm 0.01$ mm^{-1} with equal probability, whenever a rod collides with the base or the lid with relative velocity v_{rel} of contact points normal to contact plane, and the value 0.01 is chosen to reproduce the observed orientational diffusion. We set the values of friction and restitution coefficients μ and e to 0.05 and 0.3 for particle-particle collisions, 0.03 and 0.1 for rod-base collisions, 0.01 and 0.1 for rod-lid collisions and 0.03 and 0.65 for particle-V collisions respectively, to match the experiments as best we can. The ballistic dynamics of the particles is governed by Newtonian rigid body dynamics. VMD software [19] is used to make all movies and snapshots from simulations.

Fig. 1(a) and (c) show the configuration of rods below and above the critical angle in experiments (See supplementary video 2). Fig. 1(b) and (d) show the corresponding picture in simulation, with system size of 39ℓ (supplementary video 3).

In order to quantify trapping, we calculate the instantaneous speeds of all the particles in every frame and track the number N_0 at zero velocity. We plot the trapping efficiency $\eta \equiv N_0 a/A_t$, where a is the area of the two-dimensional projection of the rod on the surface. We find that this quantity drops abruptly at $\theta = 120°$ in ex-

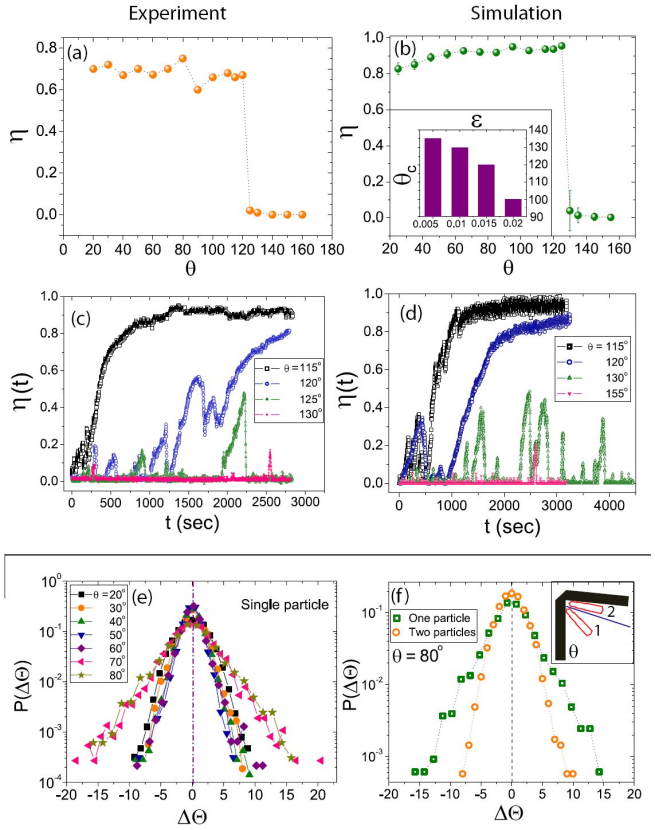

FIG. 2: Trapping efficiency shows a sudden jump at $\theta = 120°$ for (a) experiment and (b) simulation, indicating a trapping to detrapping transition. The critical transition angle decreases monotonically with angular noise as shown in the inset to (b). Close to the transition angle, we see repeated attempts where rods tend to form metastable structures inside the trap which become increasingly rare as we move away from the transition angle, for both experiment (c) and simulation (d). (e) Probability distribution of angular fluctuations of single rod inside a trap. The transition angle of escape for one rod is 70° at and beyond which the particle begins to show enhanced angular fluctuations. (f) Introduction of second rod suppresses the width of the distribution which leads to a trapped state. (Inset) A schematic of two rods in a trap.

periment and $\theta = 125°$ in the simulation (Fig 2 (a) and (b) respectively). We study the effect of angular noise on the threshold angle θ_c below which trapping occurs. We find a monotonic decrease of θ_c with increasing angular noise ε; see inset to Fig. 2(b). Beyond $\varepsilon = 0.02$ mm^{-1} it is hard to observe trapping at any θ.

We have run longer experiments (45 min) and simulations at trap angles $115°, 120°, 125°$ and $130°$. We plot the time-evolution of η in experiment Fig. 2(c) and simulation Fig. 2(d). For both experiment and simulation, with $\theta = 115°$, η increases monotonically with time and saturates to a value close to 0.9. At 120° in the experiment the system displays multiple attempts, one of which leads to trapping. At somewhat larger θ in simulation and experiment such peaks in $\eta(t)$ are seen but are ultimately unsuccessful. These nucleation-like events together with the abrupt onset as a function of θ are indications of an underlying discontinuous nonequilibrium trapping phase transition.

We turn now to the relation between single-particle and collective trapping. In Fig. 2(e) we plot the probability distribution of angular fluctuations between two frames, i.e. P($\Delta\Theta$) where $\Delta\Theta(t)$ is the difference between the orientation of the rod in two successive frames (separated by 0.07 s). We find that for $\theta = 70°$ and $80°$, the width of the distributions is much larger than at smaller angles. We see that a single rod is trapped for $\theta \leq 70°$ (see supplementary video 4) for the duration of the experiment [20], and escapes for larger θ (supplementary video 5).

Still at $\theta = 80°$, we introduce a second rod [see inset to Fig. 2(f)]. Interestingly, the particles cooperatively trap each other, each suppressing the angular fluctuations of the other [Fig. 2(f) and supplementary video 6]. Physically, the effective trap angle seen by each rod is less than the imposed θ, thereby preventing escape, as captured by the difference in the probability distribution $P(\Delta\Theta)$ for two cases in Fig. 2(f). A naïve extrapolation suggests that as the number of particles is increased, a substantially larger θ should suffice to collectively trap a nonzero fraction of the rods. We do not however have

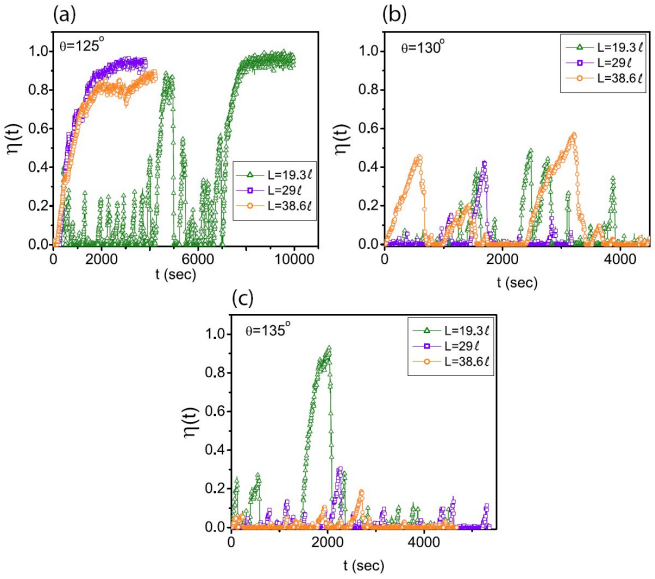

FIG. 3: (a) In a trapped state at angle $\theta = 125°$. The value of $\eta(t)$ saturates to a constant value faster for bigger systems. (b) In untrapped state near the phase boundary (at $\theta = 130°$). The value of $\eta(t)$ fluctuates above zero but the height and the duration of spikes increases with systems size. (c) In untrapped state at $\theta = 135°$. The height of spikes decreases with systems size.

a calculation that says that this threshold θ_c saturates around 120°.

To explore system-size dependence, of relevance to the question of whether the phenomenon is indeed a phase transition, we consider trap arm lengths $L = 19.3\ell, 29\ell$ and 38.6ℓ, proportionately scaling base area and number of rods. The simulations were run for three values, below ($\theta = 125°$), above (135°) and close to the transition (130°). From the plot of η as a function of time in Fig. 3 we see many failed nucleation attempts for $L = 19.3\ell$, whereas for $L/\ell = 29$ and 38.6 the trapping order parameter rapidly reaches a robust steady state value with fluctuations suppressed. This suggests a phase transition in the large$-L$ limit.

It was remarked in ref. [16] that increasing angular noise favours escape from the trap. Such noise could enter in the form of run-and-tumble behaviour, conventional angular diffusion and/or translational diffusion. In our experiments, the noise depends in detail on particle shape. Given the sensitivity of trapping to these differences in particle properties, we ask whether a trap can sort particles based on their activity. We therefore introduce another active polar rod [see Fig. 4 (a)]. This particle is 3.5 mm long and 1.1 mm thick at its thicker end, and tapered in a single step, and displays dynamics qualitatively different from that of the particles (hearafter type A) discussed in the first part of this paper. Fig. 4 (b) shows a typical trajectory of this particle (see supplementary video 7), displaying rapid directed *runs* interrupted by abrupt *tumbles* following which a new run direction is selected at random. In what follows we will refer to these as RnT particles although, unlike in bacteria [21, 22], the tumbles here are generally longer than the runs. The insets to Fig. 4(b) show a typical time-trace of V_x, the instantaneous velocity component along the long axis, and the probability distribution $P(V_x)$. Note the strongly bimodal character of $P(V_x)$, with a sharp peak corresponding to the run motion. Experiments similar to those discussed above show that our RnT particles are not trapped for any θ.

We now introduce an initially homogeneous mixture of 150 type A and 225 RnT particles into the sample cell containing a trap with $\theta = 70°$. Upon vertical shaking we find a strongly selective trapping of only the A particles, with RnT entering and leaving freely. The four images in time sequence in Fig. 1(e) illustrate this separation, and the supplementary video 8 shows the kinetics in detail.

In order to study what aspect of shape or kinetics governs the relative susceptibility to trapping, we carry out simulations in which we have independent control over particle properties. We do not attempt to recreate the complex dynamics of the RnT particles. We retain the shapes of the A and RnT particles, but force them with angular white noise. We keep the A particle noise at levels consistent with the experiment, and vary the noise strength on the RnT particles. As seen in Fig. 4(c), (d) and (e) (and supplementary video 9) for zero noise, intermediate noise and high noise respectively, the sorting is highly effective in all cases, with no perceptible effect due to the angular noise on the RnT. This is presumably a consequence of the sensitivity to initial conditions of their deterministic dynamics, through the interplay of

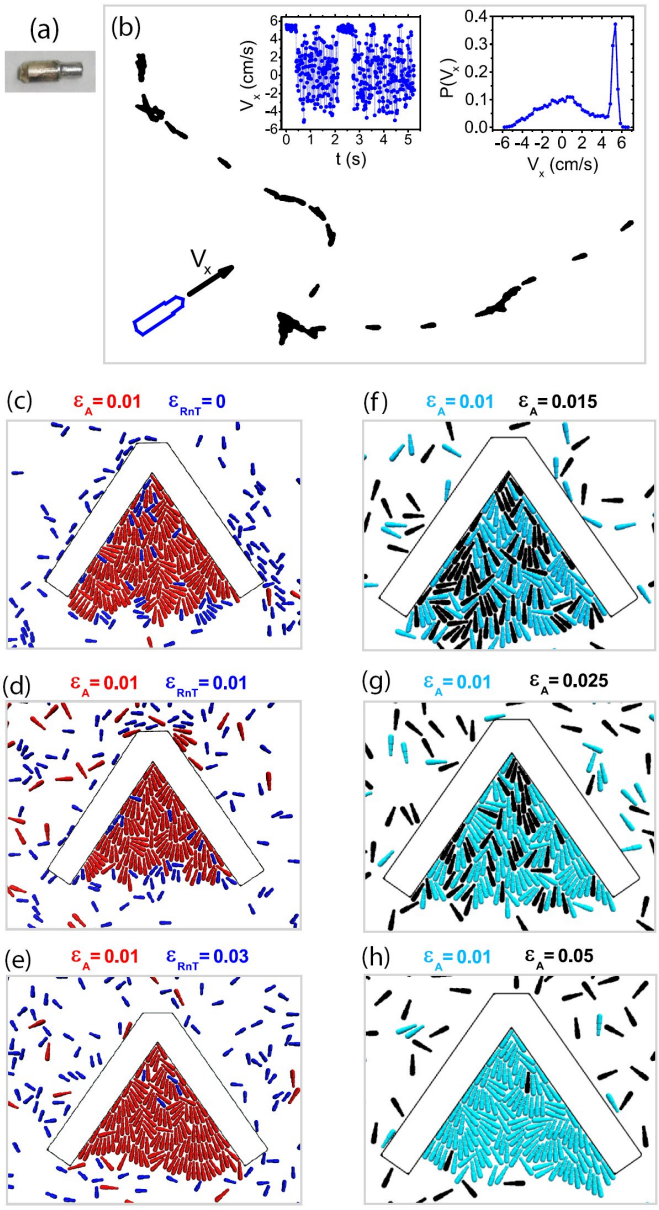

FIG. 4: (a) A photograph of the RnT particle along with its x-component of the in-plane velocity V_x and orientation θ. (b) A typical trajectory of the particle showing run and tumble events with time. Plot of V_x as function of time and its probability distribution in the inset. (c,d,e) Snapshots of steady states of mixture of A and RnT for constant ϵ_A and different ϵ_{RnT}. (f,g,h) Typical steady states for the case when angular noise is imposed selectively on particles A.

agitation, shape and interaction with the bounding surfaces. This lack of persistence is what saves the RnT particles from being trapped. This is reminiscent of the escape strategy of myxobacteria [23] when near an obstacle. Lastly, we study mixtures of geometrically identical A particles, distinguished only by an imposed difference in their angular noise. Again, Fig. 4(f), (g) and (h) (and supplementary video 10), in increasing order of difference in noise strengths, show highly effective sorting at large noise difference, with the trap predominantly populated by the less noisy, more persistent component.

Thus, the trappability of a particle is linked to the persistence of its directed motion. Reducing this persistence, whether through angular noise or enhanced shuffling along the axis of the particle, facilitiates escape from the trap, and results in a preferential accumulation of persistent movers inside the trap.

In summary, our experiments and simulations find a phase transition to a collectively trapped state when a V-shaped obstacle is introduced amidst a monolayer of artificially motile macroscopic rods, as the V is narrowed or the angular diffusion of the rods reduced. Particles with highly directional motion are preferentially trapped; a mixture of particles with different motility characteristics is thus spontaneously sorted, concentrating persistent movers inside the trap and noisy particles outside. We offer a qualitative understanding of these phenomena, but a detailed theory of trapping and sorting as possible nonequilibrium phase transitions remains to be formulated.

For support, N.K. thanks the University Grants Commission (UGC), India, H.S. thanks the Council of Scientific and Industrial Research (CSIR), India, and A.K.S. and S.R. acknowledge J C Bose Fellowships from the Department of Science and Technology (DST), India.

‡ On leave from the Department of Physics, Indian Institute of Science, Bangalore

[1] S. Ramaswamy, *Annu. Rev. Condens. Matter Phys.* **1** 323-45 (2010).
[2] M. C. Marchetti, J.F. Joanny, S.Ramaswamy, T. B. Liverpool, J. Prost, M. Rao and R. A. Simha *Rev. Mod. Phys.* **85** 1143 (2013).
[3] V. Narayan, S. Ramaswamy, N. Menon, *Science* **317**, 105 (2007).
[4] L. J. Daniels, Y. Park, T. C. Lubensky, and D. J. Durian *Phys. Rev. E* **79**, 041301 (2009).
[5] V. Schaller *et al. Nature* **467**, 73–77 (2010).
[6] T. Sanchez *et al. Nature* **491**, 431–434 (2012) .
[7] N. Kumar, H. Soni, S. Ramaswamy and A. K. Sood, *Nature Communications* **5**, 4688 (2014).
[8] V Narayan, PhD thesis, Indian Institute of Science, 2009; see chap. 5 for studies on polar particles.
[9] D. Yamada, T. Hondou, M. Sano, *Phys. Rev. E* **67** 040301 (2003).
[10] N. Kumar, S. Ramaswamy and A. K. Sood *Phys. Rev. Lett.* **106** 118001 (2011).
[11] N. Kumar, H. Soni, S. Ramaswamy and A. K. Sood *Phys. Rev. E* **91**, 030102(R) (2015).
[12] P Galajda, J Keymer, P Chaikin, R Austin, J Bacteriol. **189** 8704-7 (2007)
[13] A. Kudrolli, G. Lumay, D. Volfson and L. S. Tsimring, *Phys. Rev. Lett.* **100** 058001 (2008).
[14] J. Deseigne, O. Dauchot and H. Chaté, *Phys. Rev. Lett.* **105** 098001 (2010).
[15] He Li and H. P. Zhang, *EPL* **102**, 50007 (2013).
[16] A. Kaiser, H. H. Wensink and H. Löwen, *Phys. Rev. Lett.* **108**, 268307 (2012).
[17] http://harrypotter.wikia.com/wiki/Sorting_Hat
[18] W.S. Rasband, ImageJ, U. S. National Institutes of Health, Bethesda, Maryland, USA, http://rsb.info.nih.gov/ij/, 1997-2009.
[19] Humphrey, W., Dalke, A. & Schulten, K., VMD -Visual Molecular Dynamics. *J. Molecular Graphics* **14**, 33-38 (1996).
[20] Our findings are consistent with a trapping of a nonzero fraction of rods in the infinite-size limit, amounting to a nonequilibrium phase transition. Whether the trapping of a single active rod is a phase transition like that of the delta-function potential in three dimensions is worth further study.
[21] H. C. Berg and D. A. Brown, *Nature* **239**, 500 (1972).
[22] H. C. Berg, *E. coli In Motion* (Springer, New York, 2004).
[23] Y Wu, Y Jiang, A D Kaiser and M Alber, Phys Biol **8**, 055003 (2011).